BIOLOGIA PLANTARUM 59 (4): 560-569, 2015 DOI: 10.1007/s10535-015-0527-9

Fate of nickel and calcium in seedlings of the hyperaccumulator *Berkheya coddii* during germination

S. GROEBER[1,2,3], W. PRZYBYŁOWICZ[3,4], G. ECHEVARRIA[1,2]*, E. MONTARGES-PELLETIER[5], A. BARNABAS[3], and J. MESJASZ-PRZYBYŁOWICZ[3]

Laboratoire Sols et Environnement, Université de Lorraine, F-54518, Vandoeuvre-lès-Nancy, France[1]
Laboratoire Sols et Environnement, INRA, F-54518, Vandoeuvre-lès-Nancy, France[2]
iThemba LABS, National Research Foundation, Somerset West 7129, South Africa[3]
AGH University of Science and Technology, Faculty of Physics & Applied Computer Science, PL-30059, Krakow, Poland[4]
Laboratoire Interdisciplinaire des Environnements Continentaux, CNRS - Université de Lorraine, F-54501, Vandoeuvre-lès-Nancy, France[5]

Abstract

Little is known about Ni storage in seeds of hyperaccumulating plants and its possible role in the first stages of plant development. The aim of this study was to determine Ni distribution in seeds and seedlings during germination and to test its role during germination with and without an external Ni supply. Field-harvested seeds from the South African Ni-hyperaccumulator *Berkheya coddii* Roessler were germinated either in Ni-free deionised water or in ultramafic soil. Sections of seeds and seedlings were analyzed using micro-proton induced X-ray emission (micro-PIXE) in order to localise Ni and other elements. Results show that high amounts of Ni were stored within the seeds. In germinating seeds, Ni was located in different parts: the lower epidermis, margins of cotyledons, and the pericarp in the micropylar area. The Ni and Ca were not mobilised during germination *sensu stricto*. Emergence of the first leaf seemed to trigger the translocation of Ni and Ca within the seedling. Besides, no effect of Ni supply from soil on its redistribution could be established for the germination stage.

Additional keywords: phytomining, micro-PIXE, elemental distribution, ultramafic soil, X-ray microanalysis.

Introduction

At very low amounts, trace elements are part of the nutrition of most plants. On the opposite, high amounts of metals/metalloids in soils are generally toxic for unadaptated plants. About 450 plant species described as hyperaccumulators have adapted to metals/metalloids: they take them up from soil and accumulate them in above-ground parts at amounts substantially higher than those in soil (Brooks *et al.* 1977, Maestri *et al.* 2010, Van der Ent *et al.* 2013). This special trait has mainly been reported for the following elements: As, Cd, Cr, Mn, Co, Ni, Cu, Zn, Se, Tl, and Pb, with sometimes co-accumulation of several elements by one single species (Reeves *et al.* 2001). Various threshold concentrations were established to define hyperaccumulation for different metals/ metalloids concerned (Van der Ent *et al.* 2013).

Such plants can be cropped on metal-contaminated sites to reduce pollutant content in soils (phytoextraction as soil remediation method) or they can be cropped on naturally metal-rich soils for the economic recovery of metals/metalloids (Anderson *et al.* 1997, Robinson *et al.* 1997). Their hyperaccumulation capacities can even be enhanced by applying plant growth regulators (Bulak *et al.* 2014). Beyond theoretical progress in plant physiology and metal homeostasis in plants, a better understanding of the specific mechanisms responsible for

Submitted 3 February 2014, *last revision* 2 February 2015, *accepted* 5 March 2015.
Abbreviation: micro-PIXE - micro-proton induced X-ray emission.
Acknowledgements: The authors greatly acknowledge the Mpumalanga Parks Boards, the Department of Water Affairs and Forestry, SAPPI and SAFCOL Forestry, for permission to access sites and all assistance. This study forms part of a research project supported by the National Research Foundation (NRF) of South Africa and the French Ministries of Research and Foreign Affairs. The financial assistance of the South African National Research Foundation (NRF) is hereby acknowledged. Opinions expressed and conclusions to them are those of the authors and are not necessarily to be attributed to the NRF. The financial support of the International Atomic Energy Agency (IAEA) is also acknowledged.
* Corresponding author, fax: (+33) 383595791, e-mail: guillaume.echevarria@univ-lorraine.fr

this unusual behaviour is needed to improve the efficiency of phytoextraction.

The South African flora is rich with five Ni-hyperaccumulator species (*Senecio coronatus*, *Senecio anomalochrous*, *Berkheya coddii*, *Berkheya zeyheri* ssp *rehmannii* var *rogersiana*, and *Berkheya nivea*) having Ni content of 0.1 % d.m. in the shoots, *i.e.* 10 to 100 times higher than what is usually found in non-hyperaccumulating plants growing on the same ultramafic soil (Van der Ent *et al.* 2013). Soils developed on such geologic formations present lack of essential elements (N, P, K, S) and unbalanced Ca:Mg ratios. They also bear a high content of Mg, Cr, Co, Mn, Ni, Fe, some of which can be relatively bioavailable (Proctor 2003, Bani *et al.* 2014). These chemical characteristics contribute to the low fertility of ultramafic soils (Proctor 2003).

Among the South African hyperaccumulators, *Berkheya coddii*, a perennial plant, stands out. High biomass production has been noted by Robinson *et al.* (1997). A very high Ni content (up to 7.6 % d.m.) was reported in leaves of field-collected plants (Mesjasz-Przybyłowicz *et al.* 2004) and in total plant dry mass (1 % d.m.; Robinson *et al.* 1997). The combination of both characteristics makes it a good candidate for phytoremediation.

Many studies focused on the localisation of the hyperaccumulated elements within a plant at mature stages with no idea of the dynamics of the elements. Among various techniques that are used to reach this goal, microanalyses using proton induced X-ray emission spectrometry (micro-PIXE; Mesjasz-Przybyłowicz and Przybyłowicz 2011) as well as scanning electron microscopy with energy dispersive X-ray spectrometry (SEM-EDXS) are widely used to establish maps of elemental distribution (Küpper *et al.* 2001, Broadhurst *et al*. 2004). Results obtained show that accumulated metals are most usually stored in the upper parts of a plant and especially in leaves. The exactly opposite pattern has been found in non-hyperaccumulating but metal tolerant species (Boyd and Martens 1992, Mesjasz-Przybyłowicz *et al.* 1994). More precisely, the leaf epidermis appears to be a metal-rich tissue in many hyperaccumulators (Mesjasz-Przybylowicz *et al.* 1994, 2001, Küpper *et al.* 2001). As one of the key issues in the understanding of hyperaccumulation, Ni transport in *B. coddii* was studied using ^{63}Ni (Anderson *et al.* 1997). This experiment showed that Ni is transported to apical leaves *via* the xylem before being partially transferred down to lower leaves through the phloem. The existence of this previous study makes *B. coddii* a perfect candidate to unravel the behaviour of Ni stored in the seed during the first stages of development. This would be a first step in our understanding of why Ni is stored in hyperaccumulator seeds. Seed formation and germination are important steps in plant life cycle, and probably more important in ultramafic environments. However, no study has ever been reported on the movement of Ni and other elements from the seeds of Ni-hyperaccumulator plants during germination. Such information prior to and following germination is important as it will lighten our understanding of seed physiology of metal hyperaccumulator plants.

The Ni has been detected in seeds of Ni-hyperaccumulators *Senecio coronatus*, *Noccea pindicum*, *Stackhousia tryonii*, *Hybanthus floribundus* subsp. *adpressus*, *H. floribundus* subsp. *floribundus*, and in *Pimelea leptospermoides* (Przybyłowicz *et al.* 1995, Psaras and Manetas 2001, Bhatia *et al.* 2003, Kachenko *et al.* 2009). The place of preferential accumulation differs from one species to another, varying from the embryo to the pericarp.

The Ca is also stored in great quantities in seeds. The role of elements, such as P and K, during germination is well known for all plants. Monitoring the mobilization of Ca and Ni during the first stages of plant germination will help understand the actual role of these two elements that are stored at a high content in seeds of many of the Ni-hyperaccumulator species known worldwide. As hyperaccumulation is a parallel evolution for many taxa worldwide, we do not know if the results for *B. coddii* will allow for generalisation for all hyperaccumulator plants.

We hypothesised that Ni accumulated in hyperaccumulator seeds plays a key role in plant germination and is mobilised early in seedling development. This would help to target a further experimental work to describe the mechanisms of Ni hyperaccumulation. Therefore, for the first time, this study monitored the spatial distribution of Ni and other elements (Ca, Fe, Mn, K, P, S) in individual tissues within the seeds of an Ni-hyperaccumulator and their fate during germination under controlled conditions. It also tested the effect of germination conditions on the pattern of localisation of these elements.

Materials and methods

Plants and treatments: *Berkheya coddii* Roessler is a herbaceous plant reaching about 1.5 m at maturity with a basal root stock. Leaves are alternate, sessile, ovate-lanceolate, pointed at the extremity and with trichomes on their margins. They are around 10 - 15 cm long and 3 - 4.5 cm wide. The inflorescence at the extremity of stems has a corymbose-like shape with a mean diameter of 5 cm and a bright yellow colour. Maximum flowering is in December. The seeds are crowned by a pappus. They are wind-dispersed from January to April (Anderson *et al*. 1997).

Soils and fruits were collected in April 2010 from several ultramafic sites (four locations) of the Barberton area (S 25° 47', E 31° 03'; Mpumalanga Province, South Africa) where various populations of *B. coddii* occur. The distance between sites varied from 10 to 30 km. Soil

samples at each of these four locations were taken and fruits were collected from 20 adjacent individuals. Germination tests were performed previously to identify which population has the highest germination rate. The germination rates were determined after 12 d on moistened filter paper in Petri dishes placed in a growth chamber (a 14-h photoperiod, 300 µmol m^{-2} s^{-1}, and day/night temperatures of 24/20 °C). They varied from 13 to 48 %, depending on the area. The population with the best germination rate (Groenvaly site) was chosen for the study. The fruits were never washed prior to any experiment to avoid loss of elements.

The soil (A horizon of hypereutric magnesic chromic Cambisol) had an elevated metal content that reflected its ultramafic origin: *i.e.*, 1 570 µg g^{-1} of Cr, 590 µg g^{-1} of Ni, and 110 µg g^{-1} of Co (Proctor 2003, Echevarria *et al*. 2006). Diethylene triamine pentaacetic acid (DTPA)-extractable Ni of this soil was moderate for the ultramafic Cambisol (*i.e.*, 21.1 µg g^{-1}). Elemental analyses were performed on these materials after $LiBO_2$ fusion and acid solubilisation using an inductively coupled plasma mass spectrometer (ICP-MS; *SARM-CNRS*, Nancy, France).

Samples (0.5 g) of collected seeds (45 mg each) were dried, ground, and mineralized by heating up to 180 °C using a *SCP Science Digiprep* (8 cm^3 of HNO_3 and 4 cm^3 of H_2O_2 per sample). The solutions were then filtered through 0.45 µm ashless filter papers. Analyses of major and minor elements were performed using an inductively coupled plasma atomic emission spectrometer (*Liberty RL Varian Sequential ICP-AES*, Varian, Palo Alto, USA).

The seeds of fruits collected from selected plants from the Groenvaly site were germinated either on an ultramafic soil with very high available Ni or on an ashless filter paper. The chosen soil was organic matter-rich, clayey, hypereutric magnesic cambic Fluvisol developed on partially alluvia of serpentinised peridotites from the Agnes Mine surroundings (Barberton area). It also hosts a population of *B. coddii*. It was selected for its high total Ni content of 3 450 µg g^{-1}, determined by ICP-AES after concentrated fluorhydric acid digestion, and DTPA-extractable Ni of 221 µg g^{-1}. All seeds were firstly shocked by cold (at 4 °C for 3 d) and then transferred into the above mentioned growth chamber. To avoid any possible contamination of the specimens, no nutrient solution was applied and deionised water was used to humidify the growing media. Based on the overall morphology, four stages were identified in the development of the seedlings: the non-germinated seed (stage I), the emerged radicle (stage II), the emerged radicle and cotyledons (stage III), and the presence of the first leaves (stage IV) (Fig. 1).

Micro-PIXE measurements on seeds and seedlings: Results presented here were obtained on seeds and seedlings grown on filter papers except for the stage IV seedlings which were grown in the soil. For unknown reasons, this stage (IV) of development could not be reached on the filter paper. Three seeds or seedlings were taken at each of those four stages and immediately cryo-fixed in liquid propane cooled by liquid nitrogen using a *Leica EM CPC* cryoworkstation (*Leica Microsystems AG*, Vienna, Austria). The specimens were then lyophilised in a *Leica EM CFD* cryosorption freeze-dryer. The program used started at -70°C and ended at -20 °C 100 h later. Various hand-sections of the freeze-dried samples were hand-cut using a stainless steel razor blade.

Sectioned specimens were mounted on aluminium target frames between two layers of *Formvar*® film. To make the surface layer conductive and to prevent charge build-up during analysis, the *Formvar*® films were previously carbon-coated. Microanalyses were performed using a nuclear microprobe at the Material Research Department, iThemba LABS, South Africa. A proton beam of 3.0 MeV energy, provided by a 6.0 MV single-ended Van de Graaff accelerator, was focused to a 3.0 × 3.0 μm^2 spot and scanned over specimens using square or rectangular scan patterns with a variable number of pixels (up to 128 × 128). Scanned areas were approximately 1.0 × 1.0 mm (up to 2.7 × 2.7 mm and down to 0.4 × 0.6 mm in selected zones). The proton current was kept below 200 pA to minimize a specimen beam damage. Particle-induced X-ray emission (PIXE) and proton backscattering (BS) were performed simultaneously.

PIXE spectra were registered in the energy-dispersive mode using a Si(Li) detector (an active area: 30 mm^2, resolution: *ca*. 160 eV for the Mn Kα line) positioned at a take-off angle of 135 ° and a working distance of 25 mm. An X-ray energy range was set between 1 and 36 keV and an external absorber (125 µm Be) was positioned between the detector and the specimen to stop backscattered protons. BS spectra were recorded with an annular Si surface barrier detector (100 µm thick) positioned at an average angle of 176 °. Data were acquired in the event-by-event mode. The normalisation of results was done using the integrated beam charge, collected simultaneously from a Faraday cup located behind the specimen and from the insulated specimen holder. A more detailed description of the nuclear microprobe setup at iThemba LABS can be found in Prozesky *et al*. 1995, Przybylowicz *et al*. 1999, and Przybyłowicz *et al*. 2001, 2005.

For stages I to III, three different specimens were measured, which was a compromise between the need of replicates required to prove the reliability of results and the long beamtime needed to generate elemental maps. For stage IV, only one seedling was measured several times with the variation of an area being analysed.

Data evaluation was performed using the *GeoPIXE II* software (Ryan 2000). The PIXE spectra were fitted using a full nonlinear deconvolution procedure (Ryan *et al*. 1990a,b). Quantitative elemental images were generated using the Dynamic Analysis method (Ryan and Jamieson 1993, Ryan *et al*. 1995) and complemented with information obtained from areas selected on the basis of specimen morphology from which PIXE and BS spectra were extracted. Selection of areas was done by comparing light micrographs and the PIXE maps. The

required information on thickness and matrix composition of each area was obtained from analysis of the corresponding BS spectra using a *RUMP* simulation package (Doolittle 1986) with non-Rutherford cross-sections for C, O, and N. Errors were extracted from the error matrix generated in the fit (Ryan *et al*. 1990b), whereas minimum detection limits were calculated using the Currie formula (Currie 1968).

Results

Different tissues could be distinguished within seeds and seedlings under the light microscope (Fig. 1*A*). Fruits of *B. coddii* are typical anemochorous fruits. Seeds are enclosed in the pericarp, derived from the mother plant, which presents a special adaptation to wind dispersion (a pappus), in particular with a crown of sepals. They are composed of a seed coat surrounding an embryo in which cotyledons are predominant in volume in comparison with the other tissues, such as a pre-radicle and pre-leaf.

The total fruit elemental analysis performed using ICP-AES revealed a relatively high content of Ni and Ca [5 310 and 10 870 μg g^{-1}(d.m.), respectively], compared

Table 1. Micro-PIXE localisation of elements and their content [μg g^{-1}(d.m.)] within different tissues of a *Berkheya coddii* fruit. Means ± SE, $n = 3$. For details on Q0 - Q3, see Fig. 2.

Element	Bulk fruit (Q0)	Embryo (Q1)	Seed coat (Q2)	Micropylar area-pericarp (Q3)
Ni	4810 ± 540	4380 ± 1100	4760 ± 430	9130 ± 580
P	3220 ± 220	5570 ± 690	232 ± 71	191 ± 55
S	3000 ± 370	4390 ± 120	1500 ± 230	1158 ± 84
K	3270 ± 460	4620 ± 490	1710 ± 370	1260 ± 140
Ca	10220 ± 750	7180 ± 1150	27110 ± 1900	15590 ± 1330
Mn	84 ± 25	97 ± 26	57 ± 12	91 ± 19
Fe	48 ± 7	41 ± 2	38 ± 7	123 ± 49

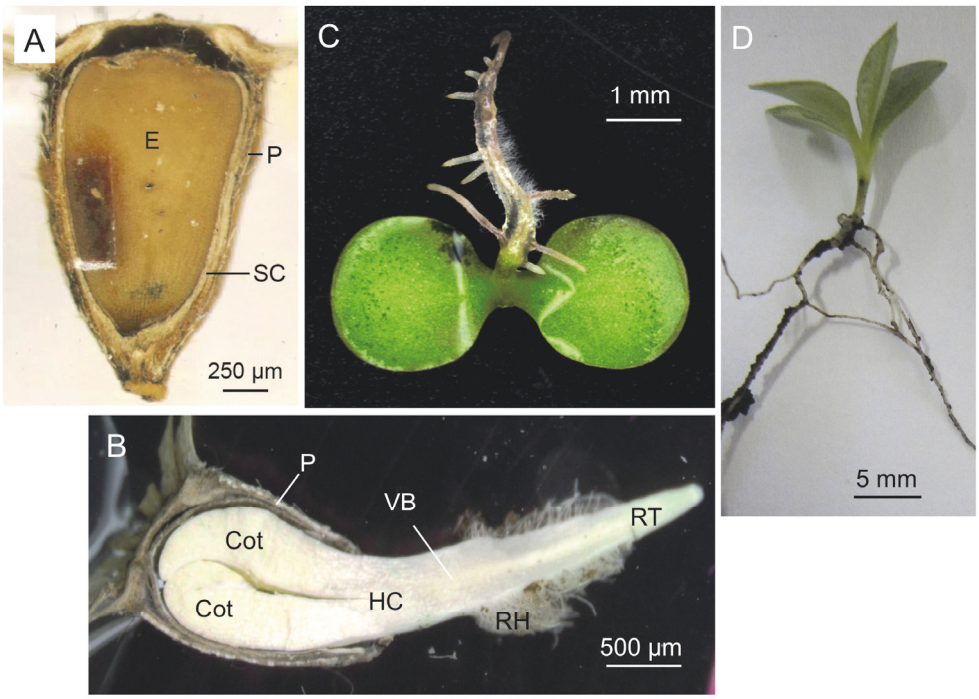

Fig. 1. Light micrographs illustrating stages in development of seedlings of Ni-hyperaccumulator *Berkheya coddii*: *A* - seed section, *B* - radicle, *C* - radicle and cotyledons, *D* - radicle, cotyledons and leaf. A darker square in the seed section resulted from prolonged PIXE measurements of this area. Cot - cotyledon, E - embryo, HC - hypocotyl, P - pericarp, RH - root hair, RT - root tip, SC - seed coat.

to other elements, such as Fe, Mn, or Mg which were 40, 84 and 1 770 µg g^{-1}(d.m.). The content of P and K in bulk fruits were 3 220 and 3 270 µg g^{-1}(d.m.), respectively.

Micro-PIXE detected the following elements at stages I to IV in *B. coddii*: Al, Si, P, S, Cl, K, Ca, Cr, Mn, Fe, and Ni. A sporadic presence of Cu, Zn, As, Br, Rb, Sr, and Zr was also recorded. Content of the main elements in fruits of *B. coddii* is compiled in Table 1. Figs. 2 to 4 only illustrate the results for major nutrients (Ca, P, and K) and for Ni and Mn. The absence of contamination of the samples by soil particles was checked using the Si and Fe elemental maps. During germination (Fig. 3), the patterns observed for the distribution of Ni and other elements (Ca, P, and K) were not affected by the growing medium (*i.e.*, the ultramafic soil or ashless filter paper).

The element content for the whole fruits (stage I) obtained by ICP-AES (data not shown) and micro-PIXE (Table 1) were generally within the same range. The micro-PIXE results revealed that P was present in the embryo (the cotyledons, but mainly the pre-radicle) at an average content of 5 570 µg g^{-1}(d.m.). A lower content of 3 220 µg g^{-1}(d.m.) was detected in the bulk fruit. This pattern was also observed for most primary and secondary nutrients, such as K or S which were also preferentially concentrated within the embryo.

Unlike most elements, Ca was preferentially stored in the seed coat, where the content reached 2.7 % of dry mass in comparison with 1.0 % of dry mass in the bulk fruit. The average content of Ca in the fruit was more than three times higher than the content of primary macronutrients, such as P and K.

The Ni presented a specific distribution, with high content in the seed coat as for Ca but also in the bottom area of the embryo as for P and K. It was predominantly accumulated in the pericarp (the micropylar area) up to 9 130 µg g^{-1}(d.m.), at the bottom of the embryo, in the lower epidermis, and to a lesser extent in the margins of the cotyledons. The Ni content within the embryo was highly variable and showed high standard errors (Table 1). Its content in the bulk fruit [4 810 µg g^{-1}(d.m.)] and in the seed coat [4 760 µg g^{-1}(d.m.)] was similar.

The Mn content in the embryo [100 µg g^{-1}(d.m.)] was similar to its content in the micropylar area [90 µg g^{-1}(d.m.)], and it was lower in the seed coat [60 µg g^{-1}(d.m.)]. The quantitative elemental map (Fig. 2) shows that the preferential area of accumulation within

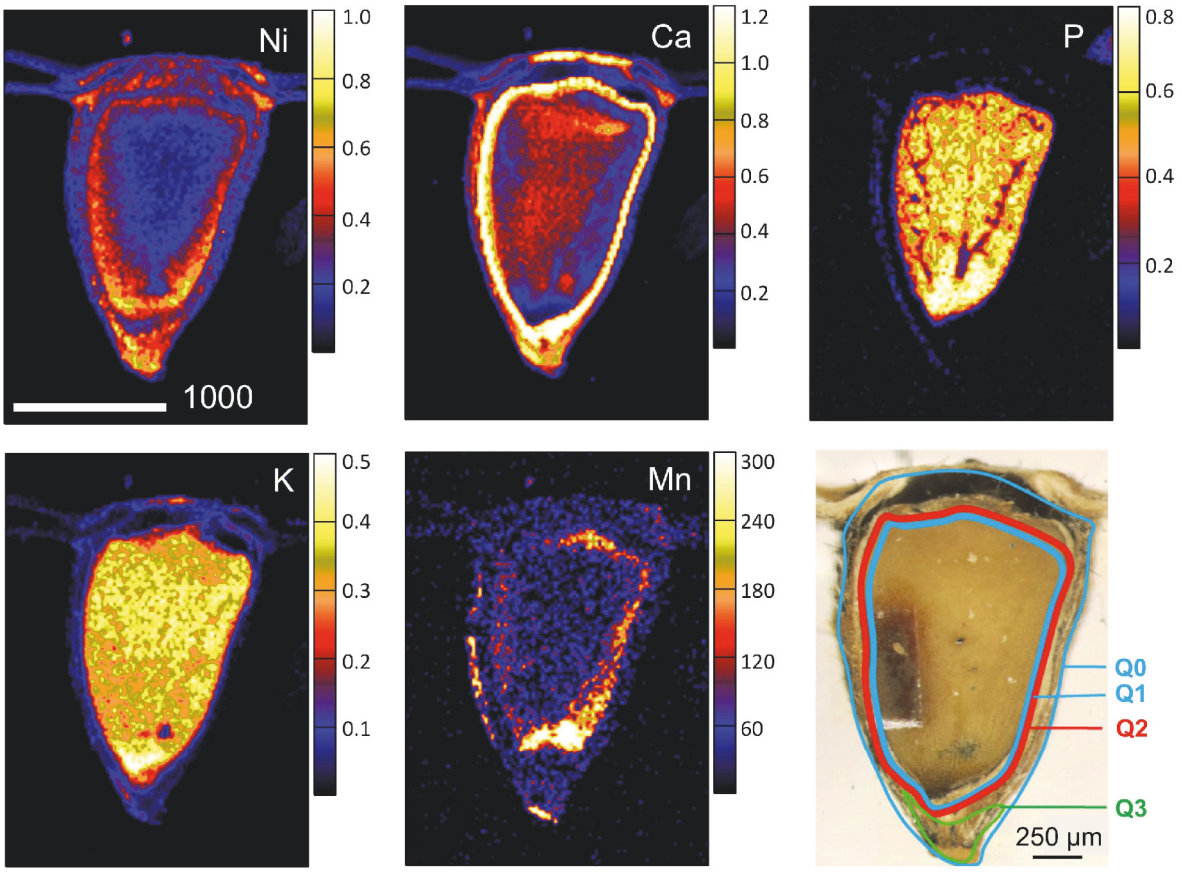

Fig. 2. Quantitative elemental maps of a sectioned seed of Ni-hyperaccumulator *Berkheya coddii*. Content in % (d.m.) or µg g^{-1} (Mn). Q0 - bulk fruit, Q1 - embryo, Q2 - seed coat, Q3 - micropylar area of pericarp. Quantitative data for the selected regions Q0 - Q3 are shown in Table 1.

the fruit was restricted to the margins of the cotyledons and to the bottom of the embryo, *i.e.*, the area of the future radicle. This is not obvious from Table 1 since the areas selected for content calculation (Q0 - Q3) covered a surface much larger than the very narrow spots of preferential accumulation.

The Fe localisation was relatively homogeneous within the fruit tissues [48, 41, and 38 μg g^{-1}(d.m.) in the bulk fruit, embryo and seed coat, respectively]. However, in the micropylar area - pericarp (Q3 in Fig. 2 and Table 1) it reached 123 μg g^{-1}(d.m.).

The localisation of Ni and Ca in the germinating seedlings of *B. coddii* (stage II, Fig. 3) did not differ from their initial localisation in the seed (stage I). Most nutrients, such as P and K, were already mobilised during this stage and their distributions were strongly modified compared to their initial localisations in the seed. The P appeared to be concentrated in the root tip where its content reached 5 295 μg g^{-1}(d.m.). Additional measurements at stage III (when both the radicle and the cotyledons had emerged from the seed coat) confirmed the pattern of localisation observed at stage II for all the elements (data not shown).

At the last stage of germination (stage IV), after the first leaves had emerged, Ni and Ca were both significantly transferred and accumulated in the leaves. The content of Ni analysed in the radicles grown on the ultramafic soil was much lower than in the other plant parts [405 μg g^{-1}(d.m.)]. The K and P showed the opposite trend as Ni or Ca with a higher content in the radicles than in the cotyledons, although the highest content was observed in the leaves. Leaf primary and secondary vascular bundles appeared to be areas of a very high K content.

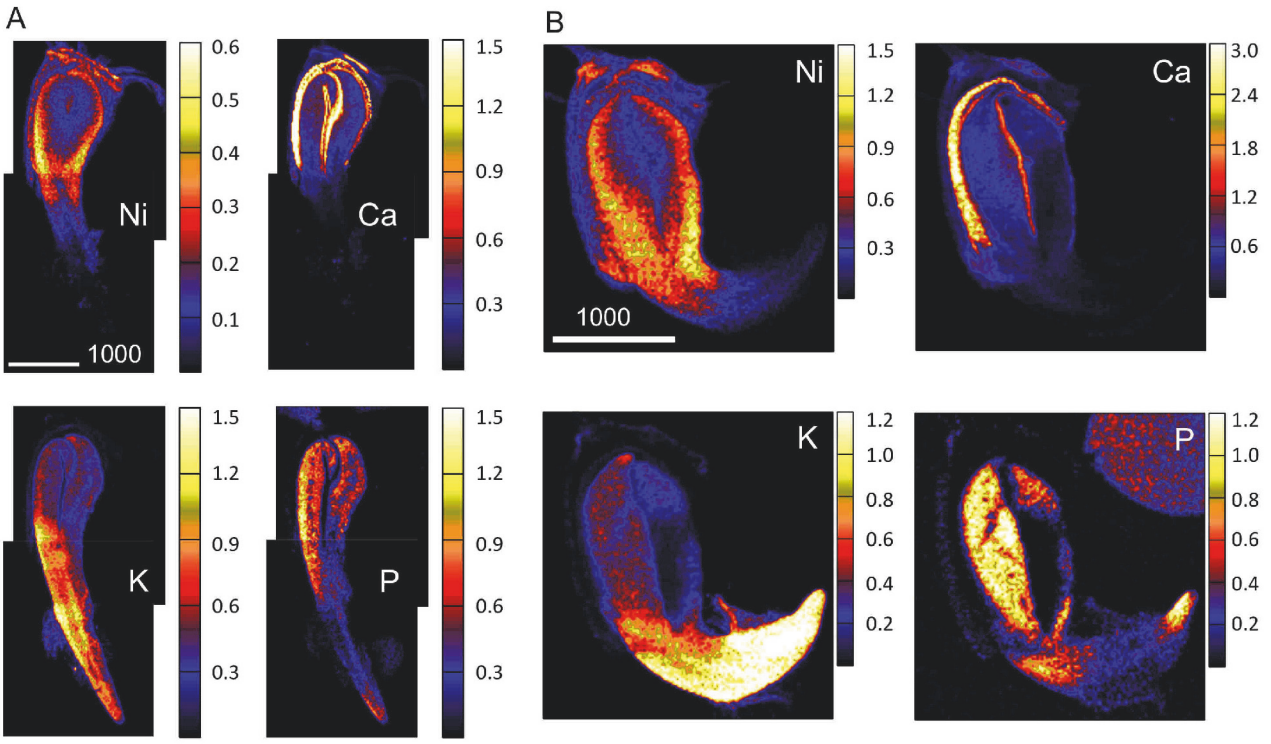

Fig. 3. Quantitative elemental maps of a germinating seedling (stage II) of Ni-hyperaccumulator *Berkheya coddii*. The comparison of two growth conditions. *A* - maps of seedling grown on Ni-rich soil (a combination of two scanned areas of the same seedling). *B* - maps of seedling grown on Ni-free filter paper. Concentrations in % (d.m.). *Scale bars* in μm.

Ni was present both in the leaves [4 860 μg g^{-1}(d.m.)] and especially in the cotyledons [7 410 μg g^{-1}(d.m.)]. Within the leaves, Ni was preferentially accumulated in the leaf margins and in the leaf midrib (Fig. 4). It was also diffusely present in the cotyledons. Ca was mostly concentrated in the midrib of the leaf as well as in the cotyledons. Neither Ni nor Ca accumulated in the leaf trichomes. As for Ni, Ca was not accumulated in the roots and root vascular bundle.

A more detailed study of the distribution of Ca, Ni, and K as well as other elements (data not shown for the maps of Cl, P, and S) was then performed on a leaf cross-section of the same seedling (Fig. 5). Ni was present both in the midrib and in the blade. In the midrib epidermis, its content reached 6 040 μg g^{-1}(d.m.), whereas it was highly depleted in the vascular bundle. In the leaf blade, Ni was mostly abundant in the palisade mesophyll [4 820 μg g^{-1}(d.m.)], and it was depleted in the secondary vascular bundle and leaf epidermis. Ca showed the same pattern as Ni. In contrast, P and K were preferentially located in the central cylinder of the midrib [2 630 and 8 395 μg g^{-1}(d.m.), respectively]. The vascular bundles in

the midrib showed accumulation of Cl, K, and P and depletion of Ca, S, and Ni. Ca and S appeared to be similarly distributed in the leaves.

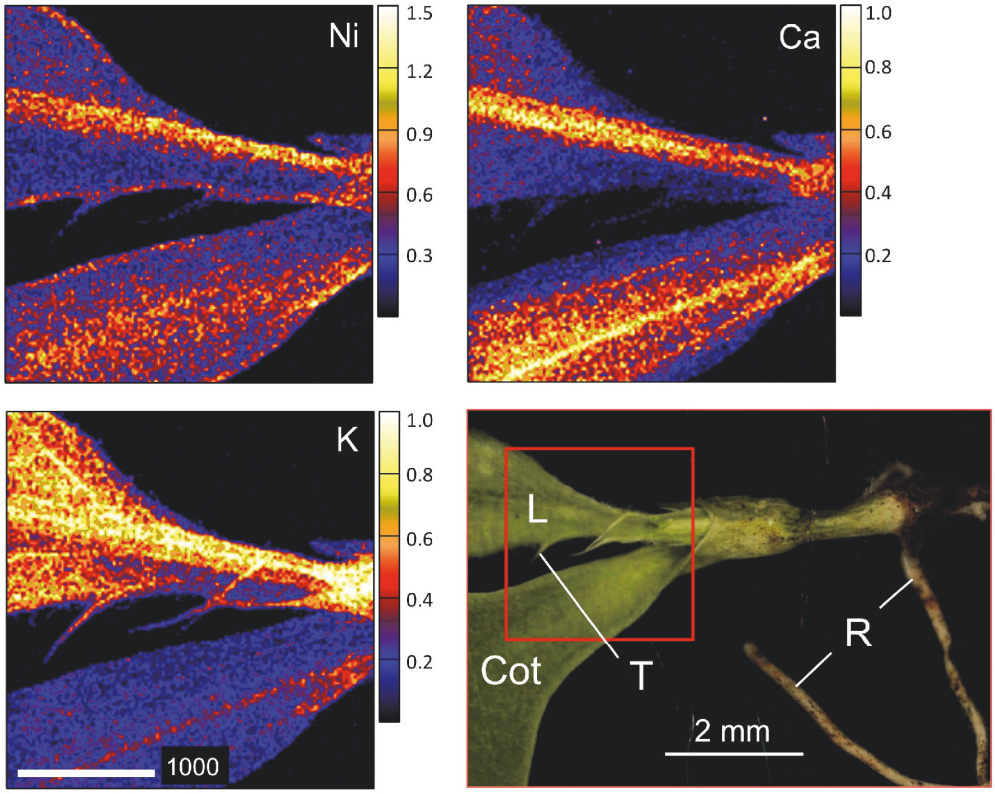

Fig. 4. Quantitative elemental maps (Ni, Ca, and K) of the last stage (IV) of a germinating seedling of Ni-hyperaccumulator *Berkheya coddii*. Content in % (d.m.). A *scale bar* in µm. A light micrograph of the same area (Cot - cotyledon, L - leaf, T - trichome, R - radicle.

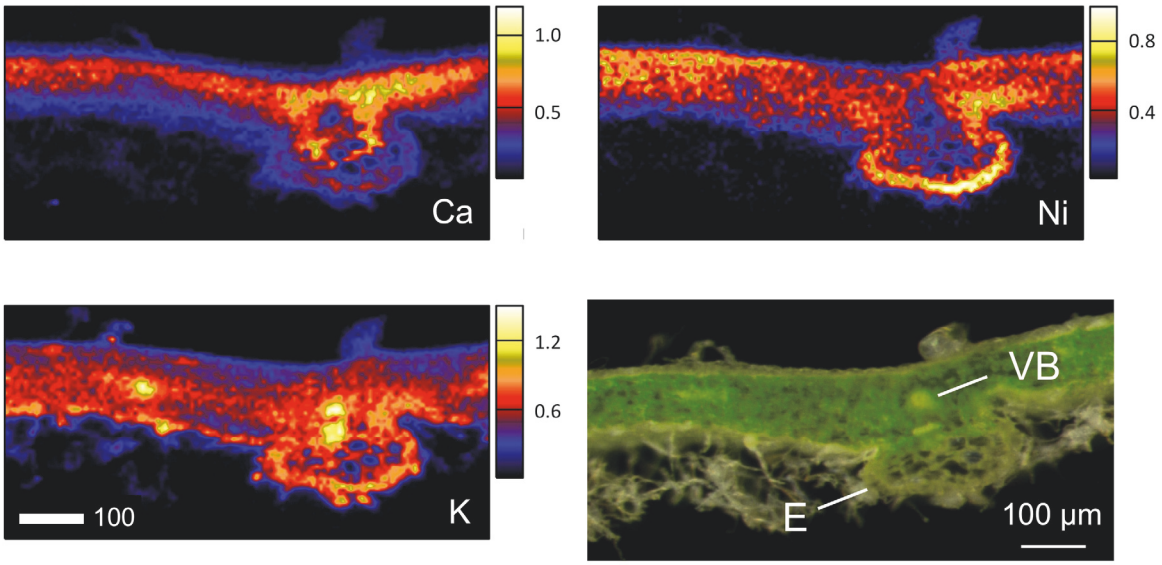

Fig. 5. Quantitative elemental maps (Ca, Ni, and K) of a leaf cross-section from the last stage (IV) of a germinating seedling of Ni-hyperaccumulator *Berkheya coddii* and a light micrograph of the same area (E - epidermis of the central midrib, VB - vascular bundle of the mid rib). Content in % (d.m.).

Discussion

The content of Ni in the bulk fruit of *B. coddii* was sometimes close to 1 % of dry mass (variation between the different populations of *B. coddii*) and was consistent with that reported in other Ni-hyperaccumulator species (Przybyłowicz *et al.* 1995, Psaras and Manetas 2001, Bhatia *et al.* 2003, Barbaroux *et al.* 2009, Kachenko *et al.* 2009). The Ca content exceeded 1 % (d.m. basis) in some cases and was surprisingly high for the plants that grew on the ultramafic soils with low exchangeable Ca:Mg ratios. For comparison, seeds, such as wheat grain, contain far less Ca [300 μg g^{-1}(d.m.)] than *B. coddii* (Vogel-Mikuš *et al.* 2009). An extreme Ca accumulation by Ni-hyperaccumulators has often been reported in previous studies (Reeves *et al.* 2007, Bani *et al.* 2009). The fate of the two elements in Ni-hyperaccumulators is somewhat linked: the plant co-accumulates them in leaf palisade parenchyma but also in seeds, probably through phloem feeding (Anderson *et al.* 1997).

Elemental maps are a clear illustration of the storage role of the embryo since most nutrients, such as P and K, were present at a relatively higher rate in this part of the seed compared to what was found in the bulk fruit. The Ca was mostly stored in the seed coat. In literature, the seed coat was also identified as a Ca-rich area for other hyperaccumulator species (*e.g.*, *Thlaspi praecox*, *Hybanthus floribundus* subsp. a*dpressus* and subsp. *floribundus*, or *Pimelea leptospermoides*; Vogel-Mikuš *et al.* 2007, Kachenko *et al.* 2009). In *B. coddii*, Ni in the pericarp was mainly concentrated in the micropylar area, which is consistent with results from other hyperaccumulators (*e.g.*, *Thlaspi pindicum* and *Senecio coronatus*: Przybylowicz *et al.* 1995, Psaras and Manetas 2001).

A drop in the content of nutrients P, S, K, and Ca in the cotyledons was observed between stage II and stage IV due to their translocation: P was evidently translocated to meristematic tissues of the root (*i.e.*, apex) where it is used for cell division. Neither Ni nor Ca was translocated during these first stages. This is different from what was observed for Cd and Zn in *Thlaspi praecox* (Vogel-Mikuš *et al.* 2007). Some generalities could be established on hyperaccumulators, but more specific aspects of their metal homeostasis seem to be particular to each hyperaccumulating plant species or taxonomic group. This explains the variety of results in the literature.

The elemental analysis conducted on the *B. coddii* seedlings at stage IV showed a clear translocation of Ni. It was also demonstrated that the content of Ni in the radicles of the stage IV seedlings grown on the Ni-rich soil was very low and similar to that in the radicles of the stage III seedlings grown in the absence of Ni, which suggests that the Ni-uptake by the root was not fully operational at this stage of development. Thus, Ni present in the leaves of the seedlings originated almost exclusively from the translocation of Ni from the cotyledons where it was originally stored. The emergence of leaves would then be the event that triggers the Ni relocation process. The fate of Ca during this stage was roughly similar to that of Ni.

In the first leaves of *B.coddii*, the lowest Ni content was found in the central cylinder of the midrib. On the contrary, the highest Ni content was found in the midrib epidermis. A hypothesis to explain this surprising depletion of Ni and Ca in the vascular tissues could be an extraordinary efficient download from the xylem and an upload in sink cells.

As for many other Ni-hyperaccumulating plant species, Ni and Ca are co-accumulated in seeds (Bhatia *et al.* 2003, Barbaroux *et al.* 2009, Kachenko *et al.* 2009). Although the benefits of plant hyperaccumulation in Ca-deficient ultramafic soils are obvious in the case of Ca, they are still discussed in the case of Ni (Boyd and Martens 1992). The storage of both elements in seeds can help a plant meet its needs at the beginning of its growth cycle before an active root uptake starts. The emergence of photosynthetic leaves is the actual start of Ni and Ca translocation in seedlings. It seems that photosynthesis of *B. coddii* directly or indirectly requires the two elements as shown by their active transport from the seed to the mesophyll (palisade parenchyma) of emerging leaves regardless of root uptake. It could be that Ni, similarly as Ca, acts as a necessary element for this plant, which would explain its storage at a high content in the seed. Its translocation to leaves at early stages of development can probably play a role in elemental defense against herbivories (Boyd and Martens 1992).

At stage IV, only one seedling was used to do repeated measurements on different areas (cotyledons, leaves, roots). Because of lack of measurements on other individuals, the interpretation of the results exposed for this stage should not be taken as generality but mostly as an indication of what occurred in that individual and it will need to be confirmed by additional measurements.

Conclusion

This work highlights that Ni and Ca accumulated in the seeds of *B. coddii* and did not participate in the development of the seedling until the first leaves were established. The obtained results suggest that the palisade parenchyma acted as Ni-sink and that the emergence of leaves activated the Ni-uptake and translocation to the storage cells. It was also established that in the first leaves of *B.coddii*, the lowest Ni content was in the central cylinder of the midrib. On the contrary, the highest Ni content was in the midrib epidermis. A reasonable hypothesis for this behaviour could be the role of Ni in the elemental defense against herbivory insects.

More comprehensive studies on other species are required to understand the role of Ni accumulated in hyperaccumulator seeds and to check whether this is a general behaviour in all hyperaccumulator species. Also, the mechanisms of Ni and Ca accumulation in flowers and seeds need a further investigation.

References

Anderson, T.R., Howes, A.W., Slatter, K., Dutton, M.F.: Studies on the nickel hyperaccumulator, *Berkheya coddii*. - In: Jaffre T., Reeves R.D., Becquer T. (ed.): The Ecology of Ultramafic and Metalliferous Areas. Pp. 261-266. ORSTOM, Paris 1997.

Bani, A., Echevarria, G., Montargès-Pelletier, E., Gjoka, F., Sulçe, S., Morel, J.L.: Pedogenesis and nickel biogeochemistry in a typical Albanian ultramafic toposequence. - Environ. Monit. Assess. **186**: 4431-4442, 2014.

Bani, A., Echevarria, G., Mullaj, A., Reeves, R.D., Morel, J.L., Sulçe, S.: Nickel hyperaccumulation by *Brassicaceae* in serpentine soils of Albania and Northwest Greece. - Northeast. Natur. **16**: 385-404, 2009.

Barbaroux, R., Meunier, N., Mercier, G., Taillard, V., Morel, J.L., Simonnot, M.O., Blais, J.F.: Chemical leaching of nickel from the seeds of the metal hyperaccumulator plant *Alyssum murale*. - Hydrometallurgy **100**: 10-14, 2009.

Bhatia, N.P., Orlic, I., Siegele, R., Ashwath, N., Baker, A.J.M., Walsh, K.B.: Elemental mapping using PIXE shows the main pathway of nickel movement is principally symplastic within the fruit of the hyperaccumulator *Stackhousia tryonii*. - New Phytol. **160**: 479-488, 2003.

Boyd, R.S., Martens, S.N.: The raison d'etre for metal hyperaccumulation by plants. - In: Baker, A.J.M., Proctor, J., Reeves, R.D. (ed.): The vegetation of Ultramafic (Serpentine) Soils. Pp. 279-289. Intercept, Andover, Hampshire 1992.

Broadhurst, C.L., Chaney, R.L., Angle, J.S., Maugel, T.K., Erbe, E.F., Murphy, A.C.: Simultaneous hyperaccumulation of nickel, manganese, and calcium in *Alyssum* leaf trichomes. - Environ. Sci. Technol. **38**: 5797-5802, 2004.

Brooks, R.R., Lee, J., Reeves, R.D., Jaffré, T.: Detection of nickeliferous rocks by analysis of herbarium specimens of indicator plants. - J. Geochem. Explor. **7**: 49-57, 1977.

Bulak, P., Walkiewicz, A., Brzezińska, M.: Plant growth regulators-assisted phytoextraction - Biol. Plant. **58**: 1-8, 2014.

Currie, L.A..: Limits for qualitative detection and quantitative determination: application to radiochemistry. - Anal. Chem. **40**: 586-593, 1968.

Doolittle, L.R. A semiautomatic algorithm for Rutherford backscattering analysis. - Nucl. Instrum. Meth. B **15**: 227-231, 1986.

Echevarria, G., Massoura, S., Sterckeman, T., Becquer, T., Schwartz, C., Morel, J.L.: Assessment and control of the bioavailability of Ni in soils. - Environ. Toxicol. Chem. **25**: 643-651, 2006.

Kachenko, A.G., Bhatia, N.P., Siegele, R., Walsh, K.B., Singh, B.: Nickel, Zn and Cd localisation in seeds of metal hyperaccumulators using μ-PIXE spectroscopy. - Nucl. Instrum. Meth. B **267**: 2176-2180, 2009.

Küpper, H., Lombi, E., Zhao, F.J., Wieshammer, G., McGrath, S.P.: Cellular compartmentation of nickel in the hyperaccumulators *Alyssum lesbiacum*, *Alyssum bertolonii* and *Thlaspi goesingense*. - J. exp. Bot. **52**: 2291-2300, 2001.

Maestri, E., Marmiroli, M., Visioli, G., Marmiroli, N.: Metal tolerance and hyperaccumulation: costs and trade-offs between traits and environment. - Environ. exp. Bot. **68**: 1-13, 2010.

Mesjasz-Przybyłowicz, J., Balkwill, K., Przybylowicz, W.J., Annegarn, H.J.: Proton microprobe and X-ray fluorescence investigations of nickel distribution in serpentine flora from South Africa. - Nucl. Instrum. Meth. B **89**: 208-212, 1994.

Mesjasz-Przybyłowicz, J., Nakonieczny, M., Migula, P., Augustyniak, M., Tarnawska, M., Reimold, W.U., Koeberl, C., Przybylowicz, W.J., Glowacka, E.: Uptake of cadmium, lead, nickel and zinc from soil and water solutions by the nickel hyperaccumulator *Berkheya coddii.* - Acta biol. cracov. bot. **46**: 75-85, 2004.

Mesjasz-Przybylowicz, J., Przybylowicz, W.J.: PIXE and metal hyperaccumulation: from soil to plants and insects. - X-Ray Spectrometry **40**: 181-185, 2011.

Mesjasz-Przybylowicz, J., Przybylowicz, W.J., Rama, D.B.K., Pineda, C.A.: Elemental distribution in *Senecio anomalochrous*, a Ni hyperaccumulator from South Africa. - S. Afr. J. Sci. **97**: 593-595, 2001.

Proctor, J.: Vegetation and soil and plant chemistry on ultramafic rocks in the tropical Far East. - Perspectives Plant Ecol. Evolut. Syst. **6**: 105-124, 2003.

Prozesky, V.M., Przybylowicz, W.J., Van Achterbergh, E., Churms, C.L., Pineda, C.A., Springhorn, K.A., Pilcher, J.V., Ryan, C.G., Kritzinger, J., Schmitt, H., Swart, T.: The NAC nuclear microprobe facility. - Nucl. Instrum. Meth. B **104**: 36-42, 1995.

Przybylowicz, W.J., Mesjasz-Przybylowicz, J., Migula, P., Nakonieczny, M., Augustyniak, M., Tarnawska, M., Turnau, K., Ryszka, P., Orłowska, E., Zubek, S., Głowacka, E.: Micro-PIXE in ecophysiology. - X-Ray Spectrometry **34**: 285-289, 2005.

Przybylowicz, W.J., Mesjasz-Przybylowicz, J., Pineda, C.A., Churms, C.L., Ryan, C.G., Prozesky, V.M., Frei, R., Slabbert, J.P., Padayachee, J., Reimold, W.U.: Elemental mapping using proton-induced X-rays. - X-Ray Spectrometry **30**: 156-163, 2001.

Przybylowicz, W.J., Mesjasz-Przybylowicz, J., Pineda, C.A., Churms, C.L., Springhorn, K.A., Prozesky, V.M.: Biological applications of the NAC nuclear microprobe. - X-Ray Spectrometry **28**: 237-243, 1999.

Przybyłowicz, W.J., Pineda, C.A., Prozesky, V.M., Mesjasz-Przybylowicz, J.: Investigation of Ni hyperaccumulation by true elemental imaging. - Nucl. Instrum. Meth. B **104**: 176-181, 1995.

Psaras, G.K., Manetas, Y.: Nickel localisation in seeds of the metal hyperaccumulator *Thlaspi pindicum* Hausskn. - Ann. Bot. **88**: 513-516, 2001.

Reeves, R.D., Baker, A.J.M., Becquer, T., Echevarria, G., Miranda, Z.J.G.: The flora and biogeochemistry of the ultramafic soils of Goiás state, Brazil. - Plant Soil **293**: 107-119, 2007.

Reeves, R.D., Schwartz, C., Morel, J.L., Edmondson, J.: Distribution and metal-accumulating behavior of *Thlaspi caerulescens* and associated metallophytes in France. - Int. J. Phytoremed. **3**: 145-172, 2001.

Robinson, B.H., Brooks, R.R., Howes, A.W., Kirkman, J.H., Gregg, P.E.H. The potential of the high-biomass nickel

hyperaccumulator *Berkheya coddii* for phytoremediation and phytomining. - J. Geochem. Explor. **60**: 115-126, 1997.

Ryan, C.G.: Quantitative trace element imaging using PIXE and the nuclear microprobe. - Int. J. Imag. Syst. Technol. **11**: 219-230, 2000.

Ryan, C.G., Jamieson, D.N.: Dynamic analysis: on-line quantitative PIXE microanalysis and its use in overlap-resolved elemental mapping. - Nucl. Instrum. Meth. B **77**: 203-214, 1993.

Ryan, C.G., Cousens, D.R., Sie, S.H., Griffin, W.L.: Quantitative analysis of PIXE spectra in geoscience applications. - Nucl. Instrum. Meth. B **49**: 271-276, 1990a.

Ryan, C.G., Cousens, D.R., Sie, S.H., Griffin, W.L., Suter, G.F., Clayton, E.: Quantitative pixe microanalysis of geological matemal using the CSIRO proton microprobe. - Nucl. Instrum. Meth. B **47**: 55-71, 1990b.

Ryan, C.G., Jamieson, D.N., Churms, C.L., Pilcher, J.V.: A new method for on-line true-elemental imaging using PIXE and the proton microprobe. - Nucl. Instrum. Meth. B **104**: 157-165, 1995.

Van der Ent, A., Baker, A.J.M., Reeves, R.D., Schat, H., Pollard, A.J.: Hyperaccumulators of metals and metalloid trace elements: facts and fiction. - Plant Soil **362**: 319-334, 2013.

Vogel-Mikuš, K., Pongrac, P., Kump, P., Necemer, M., Simcic, J., Pelicon, P., Budnar, M., Povh, B., Regvar, M.: Localisation and quantification of elements within seeds of Cd/Zn hyperaccumulator *Thlaspi praecox* by micro-PIXE. - Environ. Pollut. **147**: 50-59, 2007.